

Optimized Contrast Agent Imaging Considering Different Sources of Nonlinearity

Wilko G. Wilkening, Christian Hansen,
Christiane Fischer, Helmut Ermert

Ruhr Center of Excellence for Medical Engineering (KMR),
c/o Institute of High Frequency Engineering,
Ruhr-Universität Bochum,
Bochum, Germany

Thilo Hölscher

Department of Radiology
University of California San Diego
San Diego, USA

Abstract—So called “Low MI” imaging techniques for contrast agents limit the acoustic pressure level at the expense of signal-to-noise ratio (SNR) in order to reduce both, microbubble destruction and effects of nonlinear signal propagation in tissue (“tissue harmonics”). More than two transmissions per beam line may be required to re-gain sufficient SNR. Thus, the frame rate is reduced. If the microbubbles are not too fragile or destruction less of an issue, the generation of tissue harmonics becomes the limiting factor. We propose a nonlinear processing of echoes resulting from a two-pulse phase (pulse) inversion transmit sequence, where the original two echoes and nonlinear combinations thereof are separately filtered and then superimposed to optimally discriminate between microbubbles and tissue, even if nonlinear wave propagation in tissue is not negligible.

Keywords—contrast agents, microbubbles, nonlinear imaging, low MI, tissue, optimized filters, pulse sequences.

I. INTRODUCTION

A. Nonlinear Imaging

Today’s contrast agent imaging techniques aim at imaging the nonlinear response of microbubbles to an incident acoustic wave rather than the destruction of microbubbles. Transmitting a sequence of N coded pulses along the same beam line greatly improves and simplifies this task. For many good reasons like limited transducer bandwidth, limitation with respect to amplitude modulation, complexity of processing etc., the coding is kept simple: All N pulses have the same spectrum except for a constant phase offset (phase coding, different carrier phases) or scaling of the magnitude spectrum (amplitude coding) or a combination of both. Considering complex (analytic, baseband) echoes, the receive processing is a weighted summation, where absolute values and phases of the weights are chosen to cancel out signals resulting from linear propagation and scattering.

B. Low MI Imaging

As an acoustic wave propagates through tissue, nonlinear distortion occurs and, thus, harmonics are generated (“tissue harmonics”). The 2nd harmonic, whose center frequency equals twice the center frequency of the transmitted wave (1st

harmonic or fundamental), can hardly be distinguished from the 2nd harmonic that results from nonlinear scattering of a microbubble, although fundamental differences exist [1]. One workaround is to avoid imaging the 2nd harmonic and to rely more on the signal component that is due to a third order nonlinearity but falls into the fundamental frequency range [6]. Another option is to choose a transmit pulse coding that intrinsically suppresses the 2nd harmonic resulting from a 2nd order polynomial, i.e. e.g. a 3-pulse sequence with 0°-120°-240°-phase coding [2]. A concept that is now commonly used is to go to low acoustic pressure levels (low mechanical index), where tissue harmonics are negligible but the nonlinear response of microbubbles is already noticeable. Quite some emphasis has been put on the fact that low MI imaging does not destroy microbubbles and, thus, enables real-time perfusion imaging. A drawback, however, is the loss in SNR. To re-gain SNR, longer pulses (chirps) could be effective, since microbubbles accumulate energy, but robust signal processing is an issue [3]. The straightforward solution is to make the sequence longer. This approach reduces the frame rate and increases sensitivity to motion which has to be reduced by means of wall-filters.

II. NONLINEAR RECEIVE PROCESSING USING OPTIMIZED FILTERS

A. Processing Basics

To exemplify the processing strategy, we will consider the “vintage” phase (pulse) inversion (PI) sequence. Two pulses

$$s_1(t) = s(t), \quad s_2(t) = -s(t) \quad (1)$$

are transmitted along the same beam line. This sequence is short and well reproduced by the transmitter circuitry.

The two pulse are transmitted one after the other separated by a certain time span to allow the echoes

$$e_1(t) \text{ and } e_2(t) \quad (2)$$

to have returned to the transducer before the next pulse is transmitted. In the following, we will reset the time scale with every transmission so that $t = 0$ corresponds to the same given

Sponsored in part by the German Federal Ministry of Education and Research (Grant 13N8079).
We thank Siemens Medical Systems, Inc., Ultrasound Group for their assistance with the Axis Direct Ultrasound Research Interface.

depth for all echoes. Again for simplicity a “unity” scatterer is considered. Thus

$$e_1(t) = s(t), \quad e_2(t) = -s(t). \quad (3)$$

It is obvious that in this simple, linear case the summation of the two echoes yields

$$e(t) = e_1(t) + e_2(t) = 0. \quad (4)$$

If a nonlinear (here a quadratic) function is introduced, which in this case shall describe wave propagation or system nonlinearity, a residual signal remains:

$$\begin{aligned} e_1(t) &= s(t) + q \cdot (s(t))^2, & e_2(t) &= -s(t) + q \cdot (s(t))^2, \\ e(t) &= 2q \cdot (s(t))^2. \end{aligned} \quad (5)$$

To remove the residual signal, nonlinear combinations of the original echoes $e_1(t)$ and $e_2(t)$ are considered. These “virtual” echoes are:

$$\begin{aligned} e_3(t) &= (e_1(t))^2 = (s(t))^2 + q^2 \cdot (s(t))^4 + 2q \cdot (s(t))^3, \\ e_4(t) &= (e_2(t))^2 = (s(t))^2 + q^2 \cdot (s(t))^4 - 2q \cdot (s(t))^3, \\ e_5(t) &= e_1(t) \cdot e_2(t) = -(s(t))^2 + q^2 \cdot (s(t))^4. \end{aligned} \quad (6)$$

Because of the obvious symmetries in the original and virtual echoes, the processed echo signal $e(t)$ is accordingly calculated as

$$e(t) = e_1(t) + e_2(t) + k_1 \cdot [e_3(t) + e_4(t)] + k_2 \cdot e_5(t). \quad (7)$$

The 2nd and 4th order terms can be cancelled out by choosing

$$2q + 2k_1 - k_2 = 0 \text{ and } 2k_1 + k_2 = 0 \rightarrow e(t) = 0. \quad (8)$$

In the presence of an additional nonlinearity, i.e. scattering from microbubbles, the echo signal $e(t)$ will be non-zero.

The processing proposed above is extendible to higher orders and to amplitude coding by introducing more virtual echoes and weighting factors. It is important to note that the solution is independent of the absolute amplitude of the transmit signals. For higher orders of the polynomial, it might be necessary to choose a more complex transmit sequence in order to find non-trivial solutions for the weights.

B. Advanced Processing

Our group has previously introduced a processing scheme, where all N echoes that are acquired in response to a transmit pulse sequence consisting of N waveforms are processed by N different filters before summation, i.e. extending the weights in a weighted summation to filters [5]. These filters can compensate for inaccuracies in the generation of the transmit pulses including frequency dependent phase shifts, and they can reduce the bandwidth to ranges, where “useful” signal components are found. The block diagram is shown in Figure 1. Note that N now denotes the number of echoes, original echoes and virtual echoes, whereas the number of

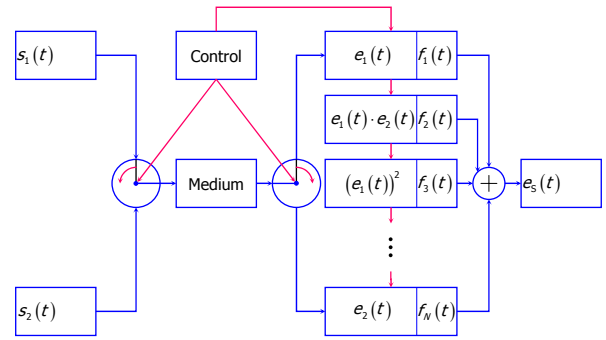


Figure 1: Block diagram of the proposed processing (nonlinear phase inversion, NL-PI). Two different pulses are sent into the medium. The resulting echoes and nonlinear combinations thereof (virtual echoes) are processed by dedicated filters prior to summation.

pulses in the transmit pulse sequences is smaller. In the following, we will only discuss the phase inversion sequence as given in (1). The combination of this sequence with the processing described above will be referred to as nonlinear phase inversion (NL-PI).

Training data representing 2 different media is required to determine the optimal filter coefficients for a given filter length. In our case, the media are tissue and contrast agent. With respect to the optimization problem, it is sufficient to have tissue with contrast agent and tissue. The calculation of the filter coefficients is found in [4] and [5].

C. Means of Quantifying the Effectiveness of the Processing

1) Contrast

To determine the filter coefficients of the filters (see Figure 1), a simple optimization criterion has to be found, i.e. the ratio of the energies in $e_s(t)$ for the 2 media. Given that the total number of filters is N and the filters shall have J taps each, these N filters will be referred to as a set of filters. The optimization process yield $N \cdot J$ complete sets representing local maxima with respect to the energy ratio.

For contrast agent imaging, contrast has to be a measure of the ability of an observer to differentiate between perfused tissue, i.e. tissue with microbubbles in the microcirculation, and unperfused tissue. Since nonlinearity is involved in the generation of the echoes and in the receive processing, the assumption that amplitudes are Rayleigh distributed does not hold. Thus, measures like the distance between amplitude distributions in dB are no applicable. Instead we define a classification error as the overlap of normalized histograms representing the amplitude distributions for the two media with respect an optimally chosen threshold. The definition is illustrated in Figure 2. We have found that for a small given number of taps J , the set of filters that gives the highest energy ratio also gives the lowest classification error. For longer filters (e.g. $J > 15$), a mismatch between the criteria was found.

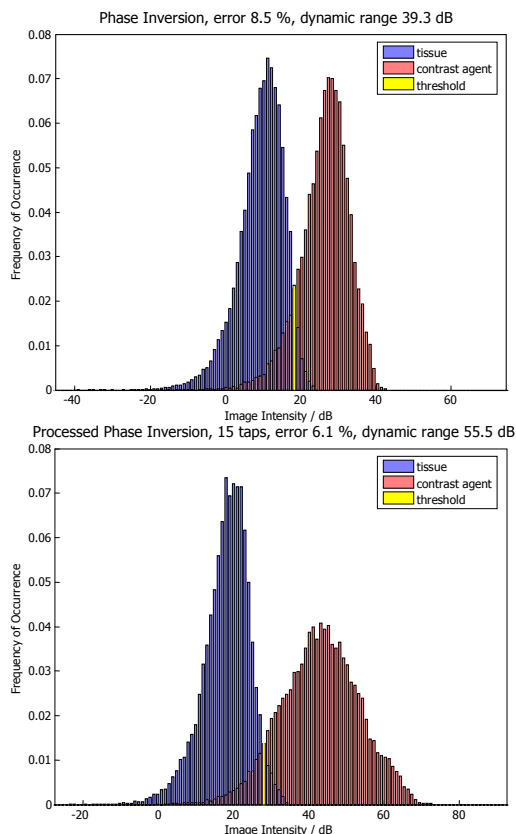


Figure 2: Histograms showing image intensity distributions of the same region in a human liver before (blue) and after (red) the injection of contrast agents for two different processing techniques. The error quantifies the percentage of misclassified pixels (overlap) according to the optimally chosen threshold (yellow). At total overlap of the histograms yields an error of 50%, where the threshold will cut the histogram in halves.

2) Axial Resolution / Bandwidth

In general, a broadband pulse is shorter in the time domain than a narrowband pulse. There are, however, some pitfalls. A short pulse and a chirp may have the same bandwidths, although the chirp is longer. A compression filter (allpass) is needed to derive a short pulse from the chirp. If we superimpose two narrowband pulses, the resulting pulse is still long and typically shows range lobes. Nevertheless, bandwidth is an indicator for axial resolution. Thus, we calculate an effective bandwidth as follows: RF data is taken from tissue with contrast agent. The spectrum of $e_s(t)$ is divided into small bands, which are then sorted by magnitude. Going from high to low magnitudes, energies in the sub-bands are added until half of the total energy is reached. The total bandwidth of these sub-bands gives the effective bandwidth.

III. EXPERIMENTAL RESULTS

A. Data Acquisition

A Siemens Sonoline[®] Antares ultrasound system equipped with the Axius Direct Ultrasound Research Interface was used to acquire RF data in vitro and in vivo. The in vitro-data are not

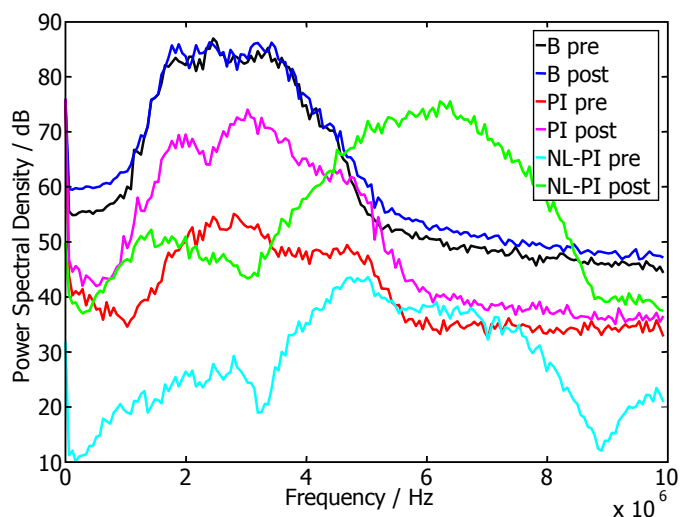


Figure 3: Spectra taken from the same ROI as used for Figure 2. B: Unprocessed RF data, contrast agent is not detectable. PI: Standard phase inversion (summation of the two echoes per beam line), strong contrast enhancement (pre \rightarrow post) in the fundamental frequency range. NL-PI: Proposed processing results in a strong contrast enhancement in the 2nd harmonic frequency range.

shown here, since in vivo data give a more realistic impression of the performance.

1) Transcranial Imaging

Transcranial imaging was performed using a 2.5 MHz phased array (PH4-1) and the contrast agent Imagent[®]. The data acquisition was started immediately after bolus injection of the contrast agent so that pre and post contrast data are available for the filter optimization. The displayed MI was 1. This value, however, does not consider the attenuation and defocusing of the skull.

2) Liver Imaging

The procedure was the same as for the transcranial data, except that a 3.5 MHz curved array (C5-2) at an MI < 0.2 and the contrast agent Sonovue[®] were used.

B. Data Processing and Analysis

The optimal filters can reliably be determined from the pre and post contrast data. To guarantee image uniformity, it turned out to be necessary to take data from several regions in lateral direction. The filters are depth dependent. Thus, the optimal solution is to generate different filters for different depths. Alternatively, training data must include different depths. In this case, the filter length J has to be increased. Energy ratios, classification errors, and effective bandwidths were calculated for all set of filters for filter length ranging from 1 to 30 taps at 40 MHz sampling rate.

Although the achievable energy ratio increases rapidly with the number of taps, the classification error does not drop as significantly. One explanation is that the ROI, which was chosen to evaluate the classification and which does not overlap with the regions that were chosen for training, may not be completely enhanced with microbubbles. Another explanation is that the processing cannot completely differentiate between the different types of nonlinearity. A

typical result is illustrated in Figure 4. The proposed processing improves the suppression of morphological information without reducing the contrast effect, see images in the first row.

The most significant difference between the standard PI and the proposed nonlinearly filtered PI is that standard PI does not actually make use of the nonlinear response of microbubbles. This becomes very evident, if we compare the spectra shown in Figure 3. While a conventional B-Mode image totally fails to detect contrast agent, PI is quite efficient, but uses the fundamental frequency range. Thus, the enhancement is most likely due to bubble displacement or destruction. Since these phenomena are not predictable in a way that the proposed filter structure could detect them, the filters detect the nonlinear response, which is revealed in the broadband response around 6 MHz in Figure 3.

IV. CONCLUSIONS

The proposed NL-PI detects the nonlinear response of microbubbles rather than other transient effects like displacement or destruction, and suppresses the nonlinear response of tissue. The training data that are needed to determine filter coefficients can be derived directly from the

data that is to be processed. Extension to more complex sequences and higher order processing will be subjects of further investigations.

V. REFERENCES

- [1] W. Wilkening, H. Ermert, V. Uhlendorf, "Analysis of Acoustical Responses of Microbubbles for the Optimization of Phase- and Amplitude-Coded Pulse Sequences," Proceedings of the IEEE Ultrasonics Symposium, 2002, 1H-3.
- [2] S. Umemura, T. Azuma, H. Kuribara, H. Kanda, "Triplet pulse sequence for superior microbubble/tissue contrast," Proceedings of the IEEE Ultrasonics Symposium, 2003, 1E-5.
- [3] J. M. G. Borsboom, C. T. Chin, N. de Jong, "Experimental validation of nonlinear coded excitation method for contrast agent imaging Proceedings of the IEEE Ultrasonics Symposium, 2002, 1H-1.
- [4] Published Application for US-Patent, 20030069504: Receive filtering and filters for phase or amplitude coded pulse sequences; April 2003; Authors: Wilko G. Wilkening, H. Ermert, B. Brendel, Z. Mao, H. Jiang.
- [5] W. Wilkening, B. Brendel, H. Jiang, H. Ermert, "Optimized Receive Filters and Phase-Coded Pulse Sequences for Contrast Agent and Nonlinear Imaging," Proceedings of the IEEE Ultrasonics Symposium, 2001, pp. 1733-1737.
- [6] P. J. Phillips, "Contrast Pulse Sequences (CPS): Imaging Nonlinear Microbubbles," Proceedings of the IEEE Ultrasonics Symposium, 2002, 1F-5.

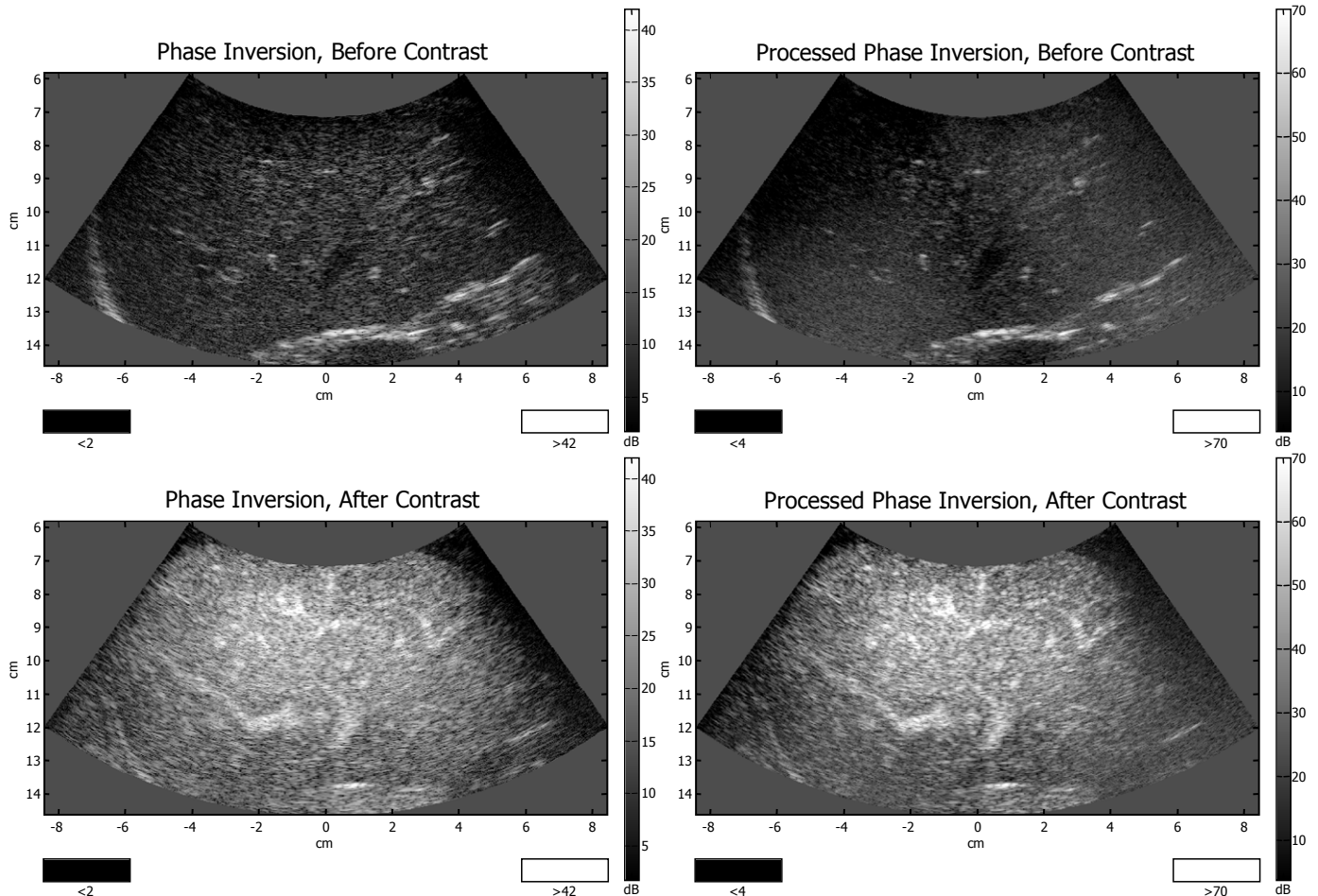


Figure 4: Images of a human liver. Left: Conventional PI. Right: Proposed processing. On a first glance, there is not a significant difference between the two columns. Note that in the pre-contrast images (top) the conventional PI shows more morphological information. Also note the finer speckle pattern in the images in the right column.

– Preprint –